Electronic Supplementary Information (ESI)

Local structure regulation of multiple upconversion emission selectivity in lanthanides highly-doped core-shell nanocrystals

Yuxuan Qiu[a], Songbin Liu[a,b*], Junjie Wang[a], Yushuang Peng[a], Yutian Yu[a], Hongyuan Fei[a], Fengli Yang[a], Jiaqing Peng[a], Junjun Tan[d], Xinyu Ye[a,c*]

a. College of Rare Earth, Jiangxi University of Science and Technology, National Rare Earth Functional Materials Innovation Center (Guorni kechuang Rare Earth Functional Materials (Ganzhou) Co., Ltd), Ganzhou 341000, P.R. China.

b. Key Laboratory of lonic Rare Earth Resources and Environment of Ministry of Natural Resources, Ganzhou 341000, P.R. China

c. Key Laboratory of Testing and Tracing of Rare Earth Products for State Market Regulation, Ganzhou, 341000, P.R. China

d. Section of Biological Chemistry, Department of Chemistry, University of Copenhagen, Universitetsparken 5, 2100 København Ø, Denmark

E-mail: songbliu@jxust.edu.cn (S. Liu); ye_xin_yu@126.com (X. Ye).

1. Theoretical analysis of upconversion process

Excitation mechanisms in upconversion systems with multiple electronic excited states are usually complex, including ground state absorption (GSA), energy transfer upconversion (ETU), luminescence, and nonradiative relaxation (NR, including multi-phonon relaxation (MPR) and cross-relaxation (CR)). Herein, we assume a simplest possible upconversion mechanism model, which is illustrated in Scheme S1 and can be simplified with six levels system.

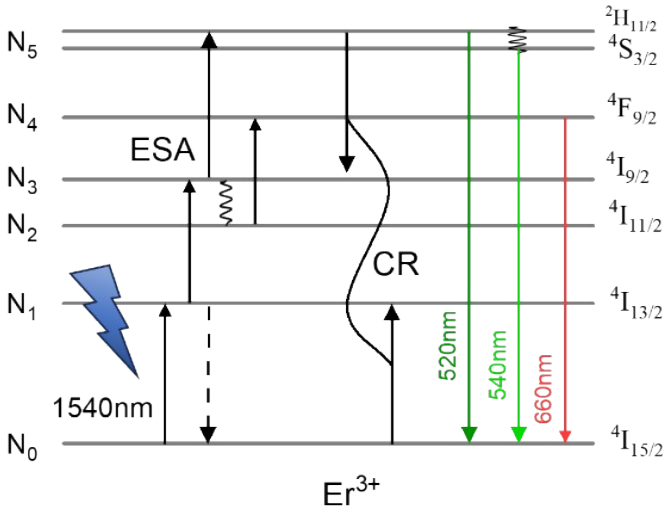

Scheme S1. Simplified five levels system in upconversion mechanism of Er^{3+} ions.

Among them, N_0, N_1, N_2, N_3, N_4 and N_5 represent the population densities of $^4I_{15/2}$, $^4I_{13/2}$, $^4I_{11/2}$, $^4I_{9/2}$, $^4F_{9/2}$ and $^4S_{3/2}$ states, respectively. The absorption coefficient R_i is the rate of the GSA and ESA processes, respectively. A_i represents the non-radiative decay rate of each energy level, and C represents the cross-relaxation (CR) rate of the transition process: $^4I_{15/2} + {}^2H_{11/2} \rightarrow {}^4I_{13/2} + {}^4I_{9/2}$. $1/\tau_i$ is related to the radiative decay rate and fluorescence lifetime of each energy level. σΦ represents the pumping rate, σ is the absorption cross section, and Φ is the excitation photon flux.

$$\frac{dN_1}{dt} = R_1N_0 - A_1N_1 + CN_0 = 0$$
$$\frac{dN_3}{dt} = R_3N_1 - A_3N_3 + CN_5 = 0$$
$$\frac{dN_5}{dt} = R_5N_3 - A_5N_5 - CN_5 = 0$$
$$N = N_0 + N_1 + N_2 + N_3 + N_4 + N_5$$

$$R_i = \sigma\Phi$$

$$A_i = \frac{1}{\tau_i}$$

1) The ground-state population density N_0 is assumed to be constant.

2) Since the excitation conditions are the same for the series of samples, the absorption coefficient R_i is related to the absorption cross section, Planck constant, and incident pump power, so it also can be regarded as constant.

3) Since the activator and sensitizer in this $LiErF_4$@$LiYF_4$ systems are Er^{3+} ion and the concentration is consistent, so cross relaxation rate C of each sample is also kept the same.

Simplify the constants and the same part of the above formula, thus,

Upconversion green emitting level: $$A_G = A_5 \propto \frac{1}{\tau_5} = \frac{1}{\tau_G}$$

Similarly:

Upconversion red emitting level: $$A_R = A_4 \propto \frac{1}{\tau_4} = \frac{1}{\tau_R}$$

In order to quantitatively analyze the influence of energy transition rate and non-radiative transition rate in series of samples, the following formulas are used:

$$\frac{1}{\tau_G} = A_{i-G} + A_{r-G}$$

$$\frac{1}{\tau_{i-G}} = A_{i-G}$$

$$\frac{1}{\tau_R} = A_{i-R} + A_{r-R}$$

$$\frac{1}{\tau_{i-R}} = A_{i-R}$$

Here τ_G, τ_{i-G}, A_{i-G}, A_{R-G} is the total lifetime, intrinsic lifetime, spontaneous emission decay rate, and the non-radiative transition decay rate of green upconversion luminescence, respectively. While τ_R, τ_{i-R}, A_{i-R}, A_{r-R} is the total lifetime, intrinsic lifetime, spontaneous emission decay rate, and the non-radiative transition decay rate of red upconversion luminescence, respectively. Therefore, we measured the intrinsic lifetime of green and red upconversion emitting level for series of samples monitored at 554 nm and 669 nm, the non-radiative transition rate was calculated by the above formulas. And the calculated results were shown in Figure. S3, Table S1 and Table S2.

We found that the non-radiative transition rate was calculated by the above formula. We found that the non-radiative transition rates of green and red light gradually decreased with the increase of CF_3COOLi amount. The calculated value of the non-radiative transition rate of the green light (A_{i-G}) is reduced from 5.80 to 4.59 $\times 10^3$ s^{-1}, while the red light (A_{i-R}) is reduced from 7.07 to 3.50 $\times 10^3$ s^{-1} for CS1 to CS5 sample, respectively. Thes results indicate that as the amount of CF_3COOLi increases, the F^- vacancy gradually decreases, and the probability of non-radiative transition gradually decreases. In turn, it affects the entire energy transition process and enhances the upconversion emission intensity. The F^- vacancy-related non-radiative transition

competes with the radiative transition, and the non-radiative transition corresponding to the red light is more suppressed than the green light, resulting in a change in the upconversion emission selectivity to exhibit multicolor upconversion characteristic.

2. Figures S1-S5

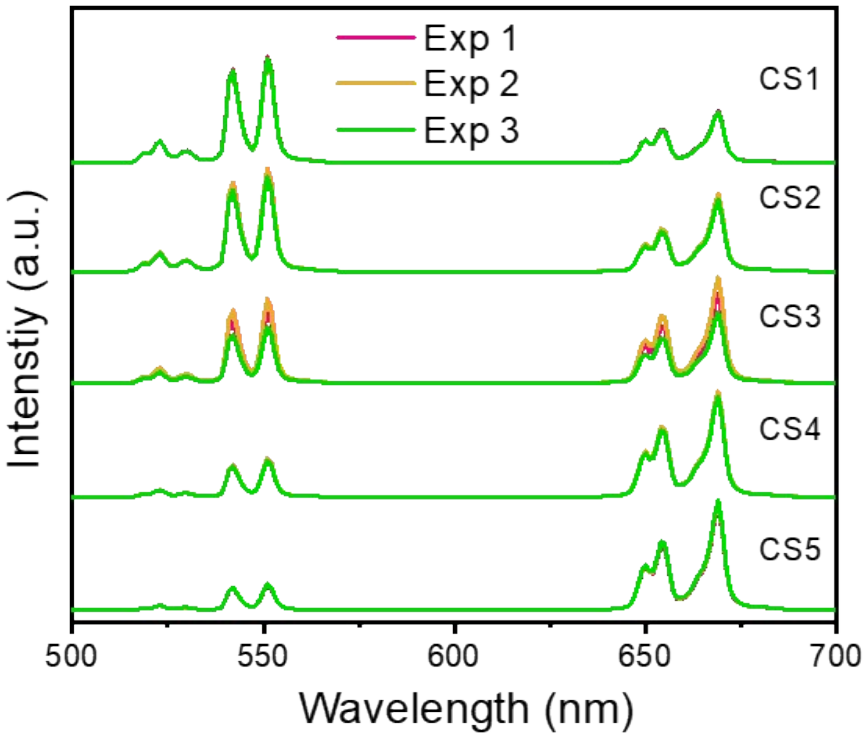

Fig. S1 Upconversion emission spectra of CS1 ~ CS5 samples with repeated same synthesis experimental procedure (Exp 1 ~ Exp 3)

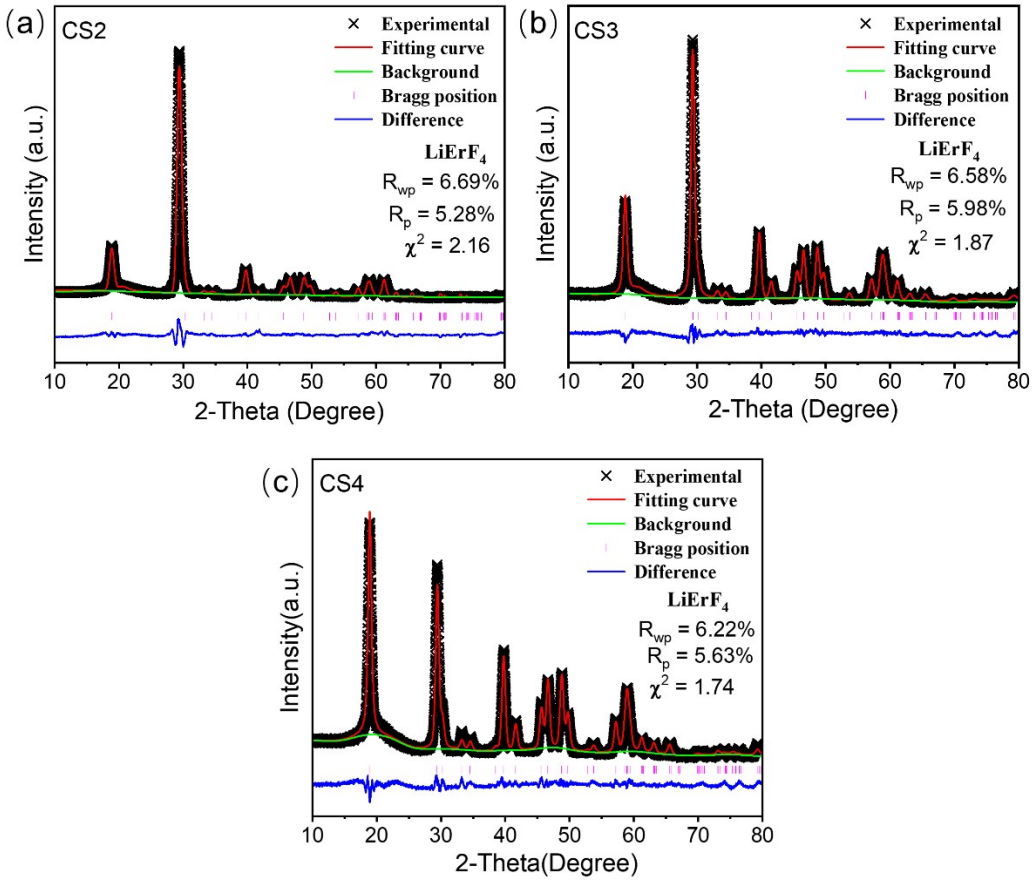

Fig. S2 XRD refinement of $LiErF_4$@$LiYF_4$ for concentration ratio of CS2, CS3 and CS4.

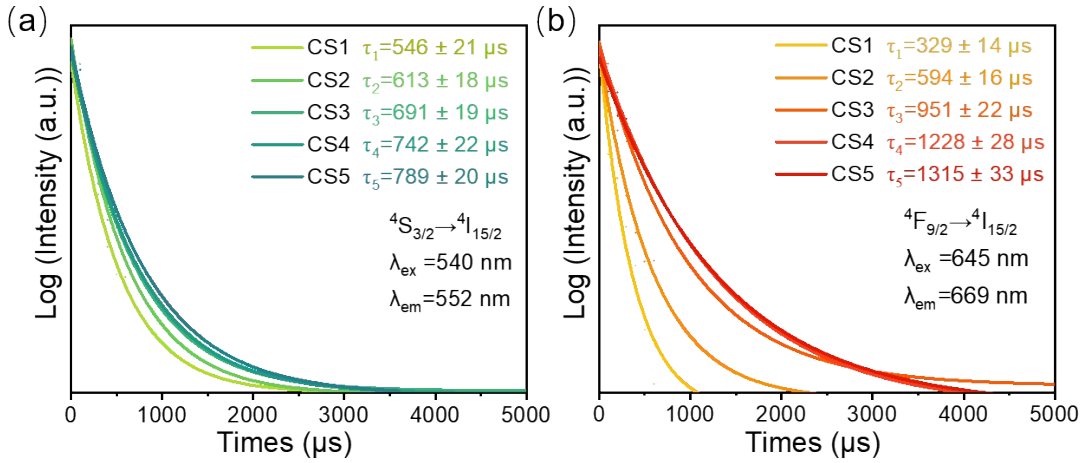

Fig. S3 The decay curves of Er^{3+} spontaneous emission for (a) green and (b) red emitting levels of $LiErF_4$@$LiYF_4$ nanoparticles

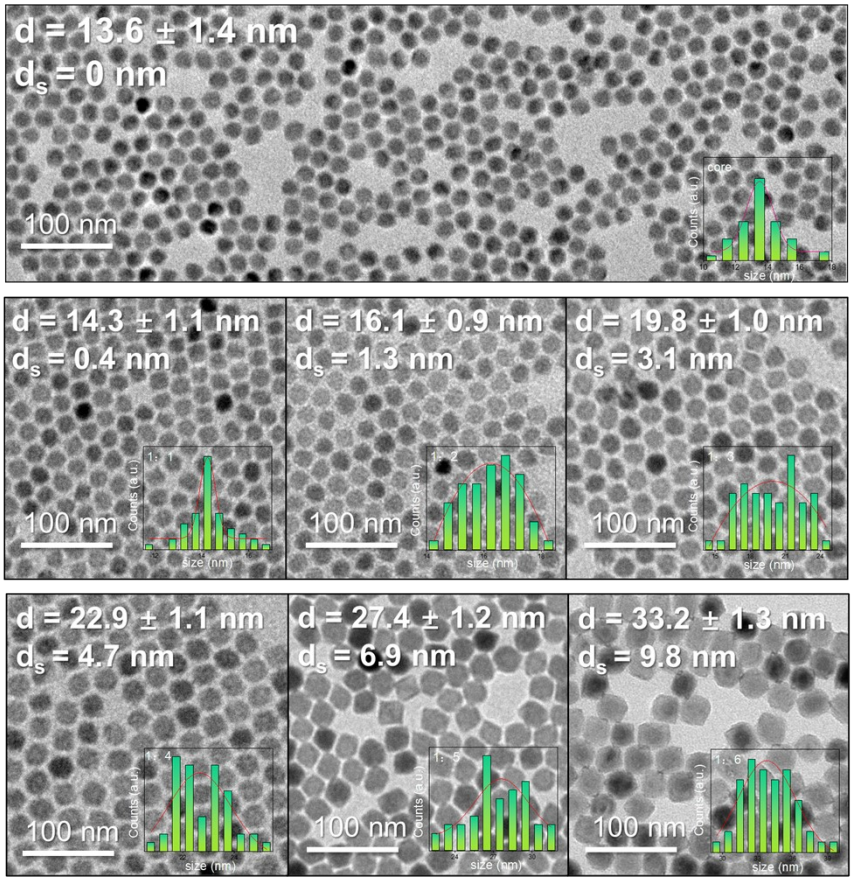

Fig. S4 TEM images of $LiErF_4$@$LiYF_4$ samples with different shell thickness, the insets show their corresponding particle size distributions.

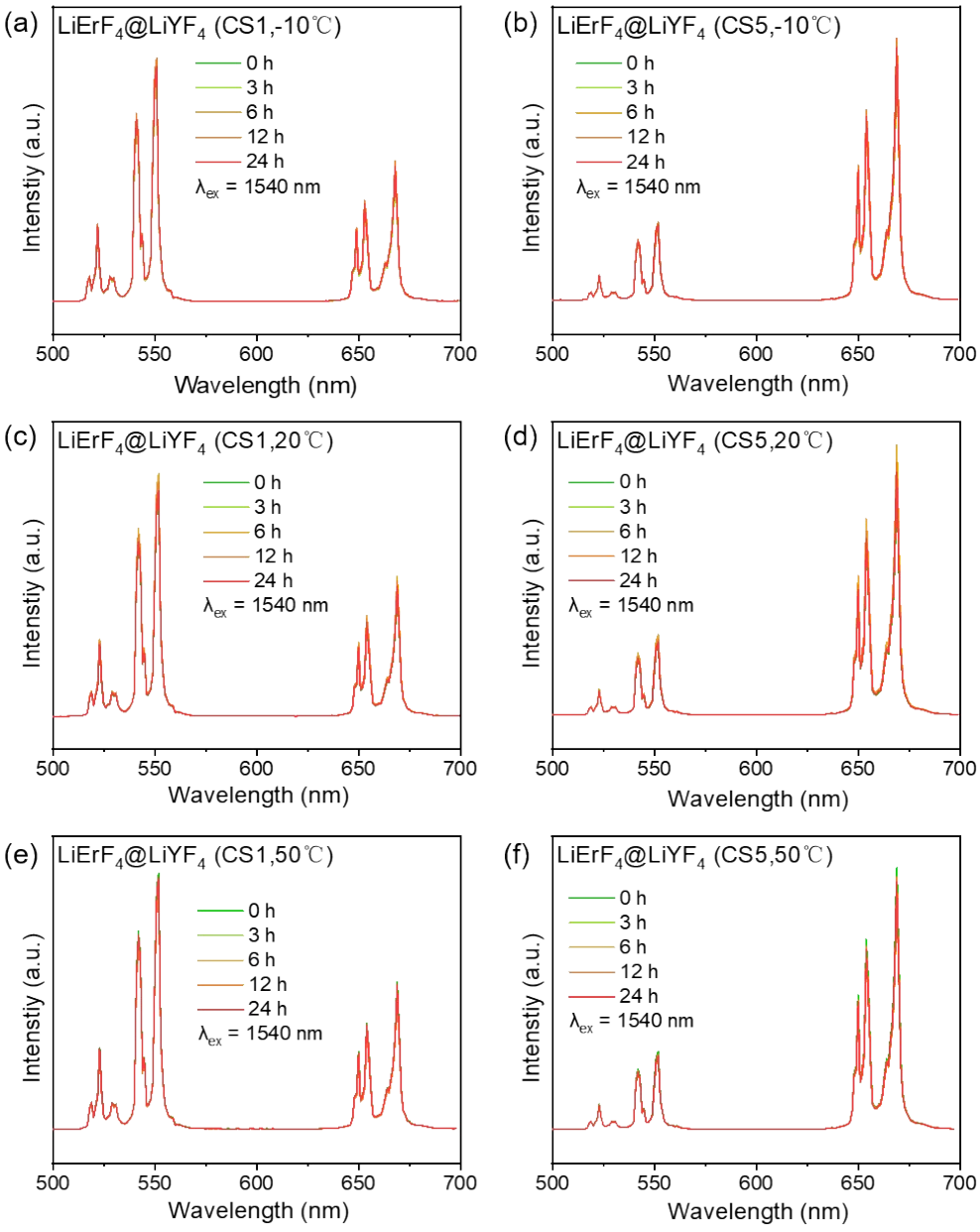

Fig. S5 (a, b) Upconversion emission spectra of CS1 and CS5 samples were measured after storage at -10°C for different time. (c, d) Upconversion emission spectra of CS1 and CS5 samples were measured after storage at 20°C for different time. (e, f) Upconversion emission spectra of CS1 and CS5 samples were measured after storage at 50°C for different time.

3. Tables S1-S3

Table S1. The calculated values of the total decay lifetime (τ_G), the intrinsic lifetime (τ_{i-G}), radiative transition rate (A_G), spontaneous emission rate (A_{i-G}), and the nonradiative transition rate (A_{r-G}) of the red light of the series of samples.

Samples	τ_G (μs)	A_G ($\times 10^3$ s^{-1})	τ_{i-G} (μs)	A_{i-G} ($\times 10^3$ s^{-1})	A_{r-G} ($\times 10^3$ s^{-1})
CS1	131	7.63	546	1.83	5.80
CS2	152	6.57	613	1.63	4.94
CS3	158	6.32	691	1.44	4.88
CS4	166	6.02	742	1.35	4.67
CS5	171	5.85	789	1.26	4.59

Table S2. The calculated values of the total decay lifetime (τ_R), the intrinsic lifetime (τ_{i-R}), radiative transition rate (A_R), spontaneous emission rate (A_{i-R}), and the nonradiative transition rate (A_{r-R}) of the red light of the series of samples.

Samples	τ_R (μs)	A_R ($\times 10^3$ s^{-1})	τ_{i-R} (μs)	A_{i-R} ($\times 10^3$ s^{-1})	A_{r-R} ($\times 10^3$ s^{-1})
CS1	99	10.10	329	3.03	7.07
CS2	148	6.76	594	1.68	5.08
CS3	196	5.10	951	1.05	4.05
CS4	226	4.42	1228	0.81	3.61
CS5	235	4.26	1315	0.76	3.50

Table S3. A comprehensive comparison of local-structure adjustable $LiErF_4$@$LiYF_4$ with other previous reported upconversion nanomaterials

Luminescence system	Modulation strategies	Upconversion enhancement factor	Upconversion R/G ratio	Overall cost	Remark	Ref.
$NaYF_4$: Yb/Er	Matrix component adjustment	2.31	0.48~6.11	Low	Changed phase, low temperature condition	[1]
$NaYF_4$: Yb/Er/Ga	Impurity ion doping	19	1~3.75	Low	No significant effect	[2]
Na_3ScF_6: Yb/Er	Particle size control	5.42	0.44~15.1	Moderation	Long time, high temperature	[3]
$Na(Y, Gd)F_4$: Yb/Er	Surface modification	1.93	4.4~6.6	High	Complex chemical operation	[4]
$NaLuF_4$: Yb/Er	Excitation sources control	/	2.69~4.96	Low	Dependent on excitation power density	[5]
$NaNbO_3$: Er/Yb	Magnetic field regulation	2.69	0.24~1.33	High	Complex magnetic field instruments and condition	[6]
$NaErF_4$@$NaYbF_4$@$NaYF_4$	Temperature field regulation	73	0.9~6.6	High	Complex temperature field instruments and condition	[7]
$NaYF_4$:Er	Electric field regulation	2400	1.02~2.12	High	Complex electric field instruments and condition	[8]
$NaYF_4$: Yb/Er	Pressure field regulation	40.32	2.4~6.1	High	Complex pressure field instruments and condition	[9]
$LiErF_4$@$LiYF_4$	Stoichiometric ratio deviation	33.37	0.53~4.55	Low	Simple synthesis operation	This work

Reference：

1. Zhang Xiang-Yu, Wang Dan, Shi Huan-Wen, Wang Jin-Guo, Hou Zhao-Yang, Zhang Li-Dong, Gao Dang-Li, *Acta Phys Sin*, **2018**, 67, 084203.
2. M. Zhang, X. Zhai, P. Lei, S. Yao, X. Xu, L. Dong, K. Du, C. Li, J. Feng and H. Zhang, *J Lumin*, **2019**, 215, 116632.

3. Y. Zhang, X. Liu, M. Song and Z. Qin, *Materials*, **2023**, 16, 2247.
4. K. Bae, B. Xu, A. Das, C. Wolenski, E. Rappeport and W. Park, *RSC Adv*, **2021**, 11, 18205–18212.
5. C. Gao, Z. Song, Y. Li, Y. Han and T. Wei, *J Fluoresc*, **2022**, 32, 1679–1684.
6. Q. Xiao, Y. Zhang, H. Zhang, G. Dong, J. Han and J. Qiu, *Sci Rep*, **2016**, 6, 31327.
7. E. Wang, W. Wang, L. Niu, Y. Feng, H. Zhao, Y. Luo, L. Zhang, Q. Li, H. Chen, Y. Chang, L. Tu, H. Zhang and J. Zuo, *Adv Opt Mater*, **2023**, 12, 5, 2301827.
8. D. Ahiboz, E. Andresen, P. Manley, U. Resch-Genger, C. Würth and C. Becker, *Adv Opt Mater*, **2021**, 9, 2101285.
9. M. D. Wisser, M. Chea, Y. Lin, D. M. Wu, W. L. Mao, A. Salleo and J. A. Dionne, *Nano Letters*, **2015**, 15, 1891–1897.